

Reversible Holographic Patterns on Azopolymers for Guiding Cell Adhesion and Orientation

Carmela Rianna,^{†,‡} Alejandro Calabuig,^{†,||} Maurizio Ventre,^{†,‡,§} Silvia Cavalli,[‡] Vito Pagliarulo,^{||} Simonetta Grilli,^{||} Pietro Ferraro,^{||} and Paolo A. Netti^{*,†,‡,§}

[†]Department of Chemical, Materials and Industrial Production Engineering, University of Naples Federico II, P. le Tecchio 80, 80125 Naples, Italy

[‡]Center for Advanced Biomaterials for Health Care@CRIB, Istituto Italiano di Tecnologia, Largo Barsanti e Matteucci 53, 80125 Naples, Italy

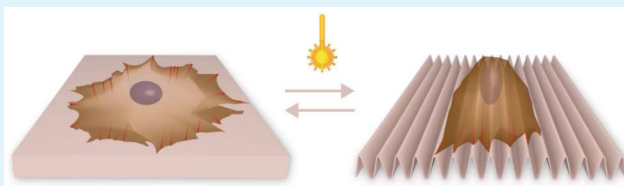
[§]Interdisciplinary Research Centre on Biomaterials, University of Naples Federico II, P. le Tecchio 80, 80125 Naples, Italy

^{||}CNR-Istituto di Cibernetica "E. Caianiello", via Campi Flegrei 34, 80078 Pozzuoli (Naples), Italy

S Supporting Information

ABSTRACT: Topography of material surfaces is known to influence cell behavior at different levels: from adhesion up to differentiation. Different micro- and nanopatterning techniques have been employed to create patterned surfaces to investigate various aspects of cell behavior, most notably cellular mechanotransduction. Nevertheless, conventional techniques, once implemented on a specific substrate, fail in allowing dynamic changes of the topographic features. Here we investigated the response of NIH-3T3 cells to reversible topographic signals encoded on light-responsive azopolymer films. Switchable patterns were fabricated by means of a well-established holographic setup. Surface relief gratings were realized with Lloyd's mirror system and erased with circularly polarized or incoherent light. Cell cytoskeleton organization and focal adhesion assembly proved to be very sensitive to the underlying topographic signal. Thereafter, pattern reversibility was tested in air and wet environment by using temperature or light as a trigger. Additionally, pattern modification was dynamically performed on substrates with living cells. This study paves the way toward an in situ and real-time investigation of the material–cytoskeleton crosstalk caused by the intrinsic properties of azopolymers.

KEYWORDS: azopolymers, SRGs, topographic patterns, reversible patterns, cell adhesion



1. INTRODUCTION

Understanding cellular reaction and response to the external environment is a central aspect in diverse biomedical, bioengineering, and clinical applications. A growing number of works emphasize the high sensitivity that cells display toward the chemical and physical features of the substrate to which they are connected. In particular, such features proved to affect different aspects of cell behavior like attachment, spreading, differentiation, and ultimately cell fate.^{1–6} Different types of signals displayed by the material substrate, such as biochemical, mechanical, and topographical signals, can influence cell behavior.^{7–10} Topographic cues are known to exert a potent influence on cell fate and functions, and many techniques were developed to fabricate micro- and nanogrooved materials to study contact guidance and mechanotransduction phenomena. The realization of substrates with topographic patterns usually relies on micro- and nanofabrication techniques, chiefly soft lithography, electron beam lithography, or focused ion beam lithography. These techniques, despite possessing a very high spatial resolution, require expensive equipment and are time-consuming, especially when large surfaces need to be processed. Additionally, once produced, the geometric features of the

master or substrate cannot be readily modified a posteriori because the displayed topography is intrinsically static in nature. To overcome the limits of a physically static system and to develop more versatile platforms, great interest has recently arisen in using stimulus-responsive materials as dynamic supports to investigate cell response.^{11,12} These works made use of temperature-responsive cell culture systems, developed through the so-called shape memory polymers. A different approach uses azopolymer-based substrates in which topographic patterns are transferred on the material surface optically. More specifically, holographic imprinting of surface relief gratings (SRGs) on azopolymer films is a promising approach for a straightforward fabrication of dynamic substrates. In fact, holographic patterns of linearly polarized light allow the realization of precise and spatially controlled gratings, while circularly polarized or incoherent light allows pattern erasure.¹³ Large-scale surface mass displacement was observed by Rochon et al.¹⁴ and Kim et al.^{14,15} who irradiated

Received: March 9, 2015

Accepted: April 15, 2015

Published: April 15, 2015

azopolymer films with an interference pattern of light. Once the sinusoidal pattern of light is in contact with the polymer, it is able to induce the formation of SRGs, in the form of topographic arrays that trace out the light intensity profile. This phenomenon has been used to realize micro- and nanogrooved polymer films, suitable in many applications, such as optics and photonics.^{16,17} Because of their versatility and intrinsic properties, azo-based materials may have a great impact in unraveling the dynamics of cell adhesion events or in inducing specific adhesion-related signaling. Indeed, few examples of SRG applications to cell cultures have been reported.^{18–20} However, studies related to dynamic pattern writing and/or erasing with living cells are lacking. On the basis of our previous experience on cell response to static micro- and nanoscale patterns,^{21–23} we explored the possibility of using light sensitive substrates to move toward the development of surfaces on which patterned signals can be manipulated dynamically. Therefore, we investigated the behavior of NIH-3T3 cells on a light sensitive azobenzene-based polymer. Surface production proved to be easy and fast, and micron-scale patterns were produced with conventional optical equipment. Polymer stability, reversibility, and dynamic writing and erasing were investigated. Elongation, orientation, and focal adhesion morphology of NIH-3T3 fibroblasts were studied on different light-induced micron-scale topographic patterns. Our data demonstrate that the process we propose is adequate for the production of material platforms to perform in vitro studies on reversible and adjustable topographic patterns. This can in principle allow investigation of cell–topography interactions and mechanotransduction in a dynamic environment.

2. MATERIALS AND METHODS

2.1. General Materials. Poly-Disperse Red 1-methacrylate (pDR1m), Triton X-100, TRITC-phalloidin, and HEPES solution were supplied by Sigma. Circular cover glasses were purchased from Thermo Scientific. Chloroform and other solvents were purchased from Romil. Anti-vinculin monoclonal antibody was supplied by Chemicon (EMD Millipore), whereas Alexa Fluor 488-conjugated goat anti-mouse antibody and ToPro3 were purchased from Molecular Probes, Life Technologies.

2.2. Substrate Preparation. Circular cover glasses (12 mm diameter) were washed in acetone, sonicated for 15 min, and then dried on a hot plate prior to the spin coating process. pDR1m was dissolved in chloroform at a concentration of 5% (w/v). The solution was spun over the cover glass by using a Laurell spin coater (Laurell Technologies Corp.) at 1500 rpm. A Veeco Dektak 150 profilometer was used to monitor the polymer film thickness. Irregular coatings were discarded.

2.3. Surface Relief Grating Inscription. A 442 nm He–Cd laser (power of ~60 mW) was used in a Lloyd's mirror configuration to project an interference pattern of light on the azopolymer films, thus inducing mass migration and SRG formation. In more detail, the azopolymer sample was glued to one of the mirror's edge and the horizontally polarized laser beam was reflected on it, thus realizing an interference pattern of light. The pattern pitch was given by $2d = \lambda \sin(\theta)$, where λ is the laser wavelength and θ is the angle between the incident beam and the mirror. With angle θ varying, patterns with different pitch could be easily prepared. Additionally, a beam from a He–Ne laser emitting at 632 nm was used for a real-time control of the inscription process by monitoring the diffraction efficiency of the inscribed grating.

2.4. Surface Relief Grating Erasure. SRG structures can be erased by subjecting them to either high temperatures or light.²⁴ Temperature-induced erasure was performed by means of a hot plate that was used to heat patterned pDR1m films up to 130 °C, a temperature that is well above the glass transition temperature of the

polymer ($T_g \sim 85$ °C). In the case of light-induced erasure, two different strategies were pursued. First, a wave plate retarder (WPR) was placed between the linear polarized beam (442 nm He–Cd laser) and the sample and acted as polarization filter, thus converting the linear polarized laser beam in a circularly polarized one. The time exposure was 10 min. When pattern erasure was performed in a wet environment, the circularly polarized laser beam was reflected with a mirror on top of a fluid-filled 35 mm diameter Petri dish. Three different fluid types were tested, namely, water, 10× phosphate-buffered saline (PBS), and Dulbecco's modified Eagle's medium (DMEM). The total fluid volume was 1.5 mL, and the time exposure was 10 min. Second, incoherent light was employed to randomize the azomolecules and erase the SRG inscription. In details, patterned samples were positioned in a Petri dish filled with aqueous solutions and irradiated from the bottom part by using a mercury lamp (15 mW intensity) with a 488 nm filter of a TCS SP5 confocal microscope (Leica Microsystems). The time exposure was 2 min.

2.5. Atomic Force Microscopy (AFM). A JPK NanoWizard II (JPK Instruments), mounted on the stage of an Axio Observer Z1 microscope (Zeiss), was used to characterize the azopolymer films in terms of surface topography and pattern features (depth and pitch). Silicon nitride tips (MSCT, Bruker) with a spring constant of 0.01 N/m were used in contact mode, in air at room temperature. The open source software Fiji²⁵ was used to measure both pattern height and pattern pitch with the 2D Fast Fourier Transform function. Five samples for each pattern type were analyzed to obtain the geometrical parameters.

2.6. Cell Culture and Immunofluorescence. NIH-3T3 fibroblasts were cultured in low-glucose DMEM and incubated at 37 °C in a humidified atmosphere of 95% air and 5% CO₂. Prior to cell seeding, pDR1m substrates were sterilized under UV light for 30 min. In principle, UV irradiation does not interfere with pDR1m conformation, because the maximum absorption band of the azobenzene polymer is 483 nm (Figure S1 of the Supporting Information). After 24 h, cells were fixed with 4% paraformaldehyde for 20 min and then permeabilized with 0.1% Triton X-100 in PBS for 3 min. Actin filaments were stained with TRITC-phalloidin. Samples were incubated for 30 min at room temperature in the phalloidin solution (1:200 dilution). Focal adhesions (FAs) were stained with vinculin. Briefly, cells were incubated in an anti-vinculin monoclonal antibody solution (1:200 dilution) for 2 h and then marked with Alexa Fluor 488-conjugated goat anti-mouse antibody (1:1000 dilution) for 30 min at 20 °C. Finally, cells were incubated for 15 min at 37 °C in ToPro3 solution (5:1000 dilution) to stain cell nuclei. A TCS SP5 confocal microscope (Leica Microsystems) was used to collect fluorescent images of cells on flat and patterned pDR1m films. Laser lines at 488 nm (vinculin), 543 nm (actin), and 633 nm (nuclei) were used. Emissions were collected in the ranges of 500–530, 560–610, and 650–750 nm, respectively. Cell and FA morphometry measurements were performed by using Fiji software. The procedure has been previously described by Ventre et al.²³ Briefly, cell elongation was assessed from phalloidin-stained cells that were analyzed with the MomentMacroJ version 1.3 script (hopkinsmedicine.org/fae/mmacro.htm). We evaluated the principal moments of inertia (i.e., maximum and minimum) and defined a cell elongation index as the ratio of the principal moments (I_{\max}/I_{\min}). In more detail, the moment of inertia of a digital image reflects how its points are distributed with regard to an arbitrary axis and extreme values of the moments are evaluated along the principal axes. High values of I_{\max}/I_{\min} identify elongated cells. Cell orientation was defined as the angle that the principal axis of inertia formed with a reference axis, i.e., the pattern direction in the case of 2.5 and 5.5 μm linear patterns and the horizontal axis (x -axis) for a flat surface and a 2.5 μm × 2.5 μm grid. Morphometric analysis of FAs was performed as follows. Digital images of FAs were first processed using a 15 pixel wide Gaussian blur filter. Then, blurred images were subtracted from the original images using the image calculator command. The images were further processed with the threshold command to obtain binarized images. Pixel noise was erased using the erode command, and then particle analysis was performed to extract the morphometric descriptors. Only

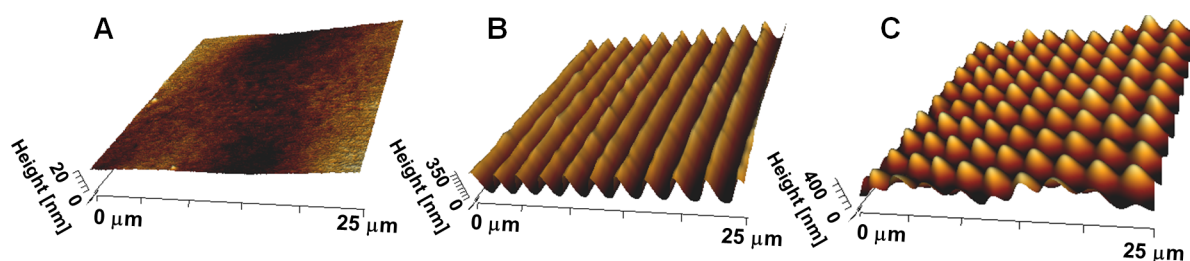


Figure 1. Three-dimensional AFM images of (A) flat spin-coated pDR1m, (B) 2.5 μm pitch pattern realized with an interference pattern of light, and (C) a 2D grating obtained by two-step illumination. The second grating was inscribed after rotating the sample by 90° .

FAs whose length was $>1 \mu\text{m}$ were included in the subsequent analysis. Significant differences between FA length or cell orientation groups were determined with the Kruskal–Wallis test run in Matlab (The Mathworks, Natick, MA).

3. RESULTS AND DISCUSSION

Azobenzene-based polymers undergo conformational changes when they are irradiated by light. More specifically, under

Table 1. Dimensions of the Geometrical Features of the SRGs

substrate	depth (nm)	pitch (μm)
2.5 μm pattern	332.9 ± 42.9	2.75 ± 0.06
5.5 μm pattern	337.9 ± 25.3	5.60 ± 0.25
2.5 $\mu\text{m} \times 2.5 \mu\text{m}$ grid	367.9 ± 101.2	2.55 ± 0.14 (vertical), 2.74 ± 0.17 (horizontal)

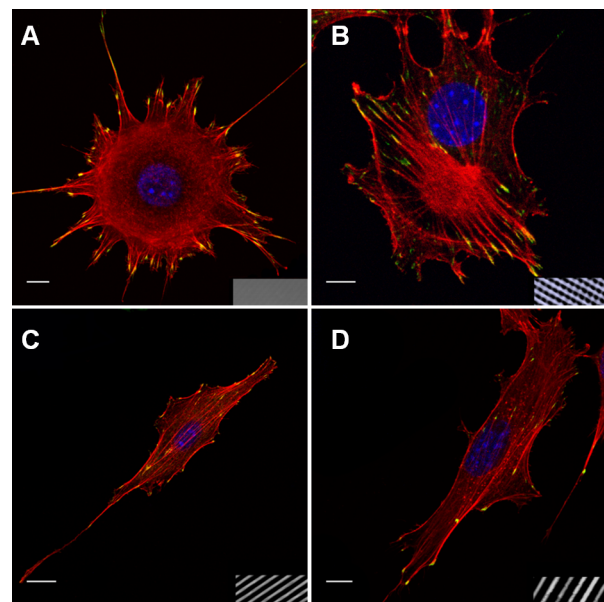


Figure 2. Confocal images of NIH-3T3 cells on (A) flat pDR1m, (B) a 2.5 $\mu\text{m} \times 2.5 \mu\text{m}$ grid pattern, and (C) 2.5 μm and (D) 5.5 μm linear patterns on pDR1m. The cell cytoskeleton is stained with phalloidin (red); FAs are immunostained for vinculin (green), and nuclei are stained with ToPro3 (blue). Transmission images of the underlying substrate are shown at the bottom right corner of each confocal micrograph. Scale bars are 10 μm .

irradiation with a proper wavelength, the continuous *trans*–*cis*–*trans* photoisomerization of azobenzene molecules, together with their change in geometrical disposition and polarity, results in a locally preferred orientation of the azobenzene groups, which direct perpendicular to the incident electrical

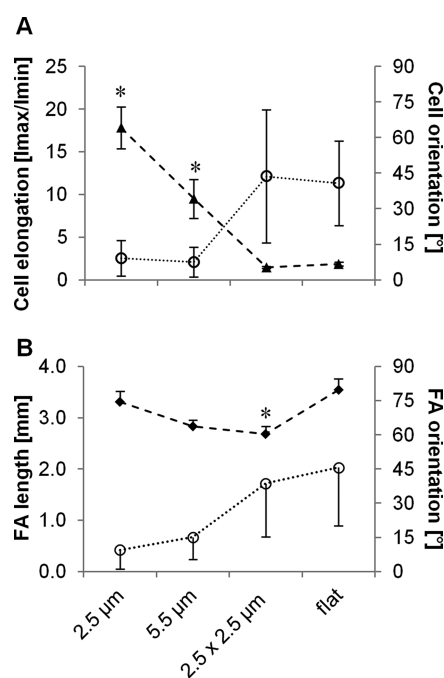


Figure 3. (A) Quantitative analysis of the cell elongation index and cell orientation on 2.5 and 5.5 μm linear patterns, a 2.5 $\mu\text{m} \times 2.5 \mu\text{m}$ grid, and flat pDR1m. Filled triangles refer to the elongation index, whereas empty circles refer to the orientation. (B) Quantitative analysis of the FA length and orientation on the substrates as in panel A. Filled diamonds represent FA length, whereas empty circles represent FA orientation with respect to the pattern direction. For the grid and flat surface, angles are evaluated with respect to the horizontal axis. The asterisk indicates significant differences with respect to the flat case ($p < 0.05$). Bars refer to the standard error of the mean for cell elongation and FA length, whereas they represent the standard deviation in the case of cell and FA orientation.

field. As a result, polymer mass migration occurs, thus inducing a pattern inscription on the material surface. Many models have been proposed so far, aiming to elucidate the mechanism of light-induced mass transport and consequent pattern formation. Among these, a thermal model,²⁶ a pressure gradient force model,²⁷ a mean-field model,²⁸ an optical-field gradient force model,^{29,30} and athermal photofluidization³¹ have been developed and presented in the past few decades. However, a general consensus about the physics that governs SRG formation has not yet been achieved. In this work, we used SRGs as cell culture substrates. Topographic patterns were inscribed and erased on pDR1m films by using an interference pattern of light and circularly polarized or incoherent beam, respectively. Because of the photoreversibility of the azopolymer surface structures, a study of the response of NIH-3T3

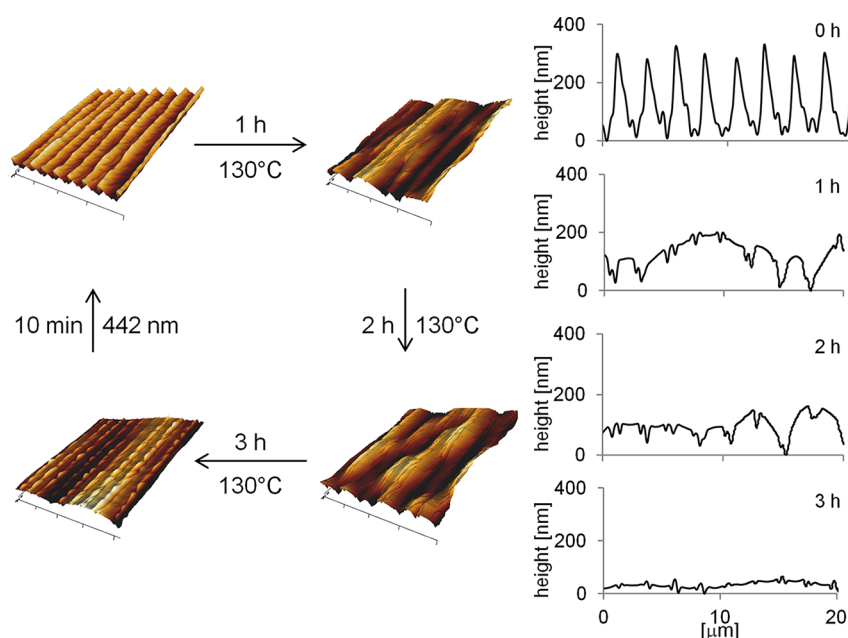


Figure 4. Three-dimensional AFM images of temperature-induced SRG erasure. The temperature was set at 130 °C for 3 h; every hour, a 20 $\mu\text{m} \times 20 \mu\text{m}$ AFM image was acquired. A SRG pattern was rewritten on the flat substrate with the Lloyd's mirror setup. On the right, height AFM cross sections are shown at different time steps.

cells to the dynamic topographic changes of SRGs was performed. Lloyd's mirror is a well-consolidated setup that we employed to realize gratings on 700 nm thick pDR1m layers (Figure 1A). In detail, a linear polarized light reflecting on a mirror resulted in a holographic pattern of light, which was able to inscribe a parallel grating on the interfering azopolymer film surface (Figure 1B). By performing a second inscription after rotating the sample by 90°, we realized a two-dimensional (2D) SRG (Figure 1C).

Patterns with different pitches were prepared by varying the angle between the laser beam and the mirror. Our study was based on linear patterns with nominal pitches of 2.5 and 5.5 μm and a two-dimensional grid with a 2.5 $\mu\text{m} \times 2.5 \mu\text{m}$ pitch. Table 1 shows the measured geometrical features of the patterns, in terms of depth and pitch.

The pattern pitch is in good agreement with the theoretical predefined values. The pitch mismatch observed on the micro grid is probably due to the imperfect overlap between the two linear patterns. In the following, substrates will be termed 2.5 and 5.5 μm linear patterns and 2.5 $\mu\text{m} \times 2.5 \mu\text{m}$ grid pattern. To use these materials as cell culture substrates, we performed a preliminary test to assess pattern stability under conditions comparable to those experienced during cell culture. Toward this aim, a 2.5 μm linear pattern was scanned via AFM, thus obtaining the time-zero height profile. Then the sample was immersed in DMEM at 37 °C for 24 h. Afterward, the sample was washed, air-dried, and scanned via AFM. The gross morphology of the pattern remained unchanged, as well as the height profile (Figure S2 of the Supporting Information), thus demonstrating the structural stability of the substrate under biological conditions. The NIH-3T3 fibroblast response to the patterned substrates was studied in terms of cell adhesion (length and orientation of FAs) and cell shape. Flat polymer films were used as control surfaces. Different topographic patterns on azopolymer films proved to exert a strong influence on cell behavior. In fact, NIH-3T3 cells were mostly round or elliptical in shape when cultivated on a flat or 2.5 $\mu\text{m} \times 2.5 \mu\text{m}$

grid pattern (Figure 2A,B), whereas they appeared to be polarized and elongated along the direction of the 2.5 μm (Figure 2C) and 5.5 μm linear patterns (Figure 2D).

This was confirmed by the quantitative image analysis performed on the confocal micrographs. In more detail, the cell elongation ($I_{\text{max}}/I_{\text{min}}$) was 17.8 ± 2.5 for cells spread on a 2.5 μm pattern and 9.5 ± 2.3 for those on a 5.5 μm linear pattern, which were significantly different from those measured on the 2.5 $\mu\text{m} \times 2.5 \mu\text{m}$ grid and flat pDR1m, i.e., 1.5 ± 0.1 and 1.8 ± 0.2 , respectively. With regard to orientation, cells were aligned in the same direction of the underlying patterns on 2.5 and 5.5 μm linear gratings, while they were randomly oriented on a 2.5 $\mu\text{m} \times 2.5 \mu\text{m}$ grid and flat polymer (Figure 3A). Our results are consistent with other reports that emphasize the role of FA assembly and orientation in cell shape and elongation.^{22,23,32}

We therefore analyzed the morphological features of FAs on the different topographies and on the flat substrate. FAs that formed on linear patterns had a comparable length that was not significantly different from that measured on the flat substrate. Furthermore, FAs on linear patterns displayed a narrow distribution of orientation angles, whose average values indicated a strong co-alignment with the pattern direction. As expected, FAs on flat substrates and on the 2.5 $\mu\text{m} \times 2.5 \mu\text{m}$ grid were randomly oriented, i.e., mean orientation of $\sim 45^\circ$, with a broad distribution. In particular, FAs on the 2.5 $\mu\text{m} \times 2.5 \mu\text{m}$ grid were significantly shorter than those on flat surfaces (Figure 3B). Therefore, it is likely that the presence of arrays of dome-shaped pillars hampers the formation of longer focal adhesions.

Thick actin bundles were clearly visible in cells cultured on linear SRG, whereas a predominant cortical actin was observed in cells on flat surfaces. Interestingly, cytoskeletal assemblies that formed in cells on the micro grid had a peculiar rosette-shaped structure. Even though confocal snapshots do not provide information about the dynamics of cytoskeleton assembly, it is tempting to speculate that as microgrids hamper FA formation, the subsequent organization of a stable

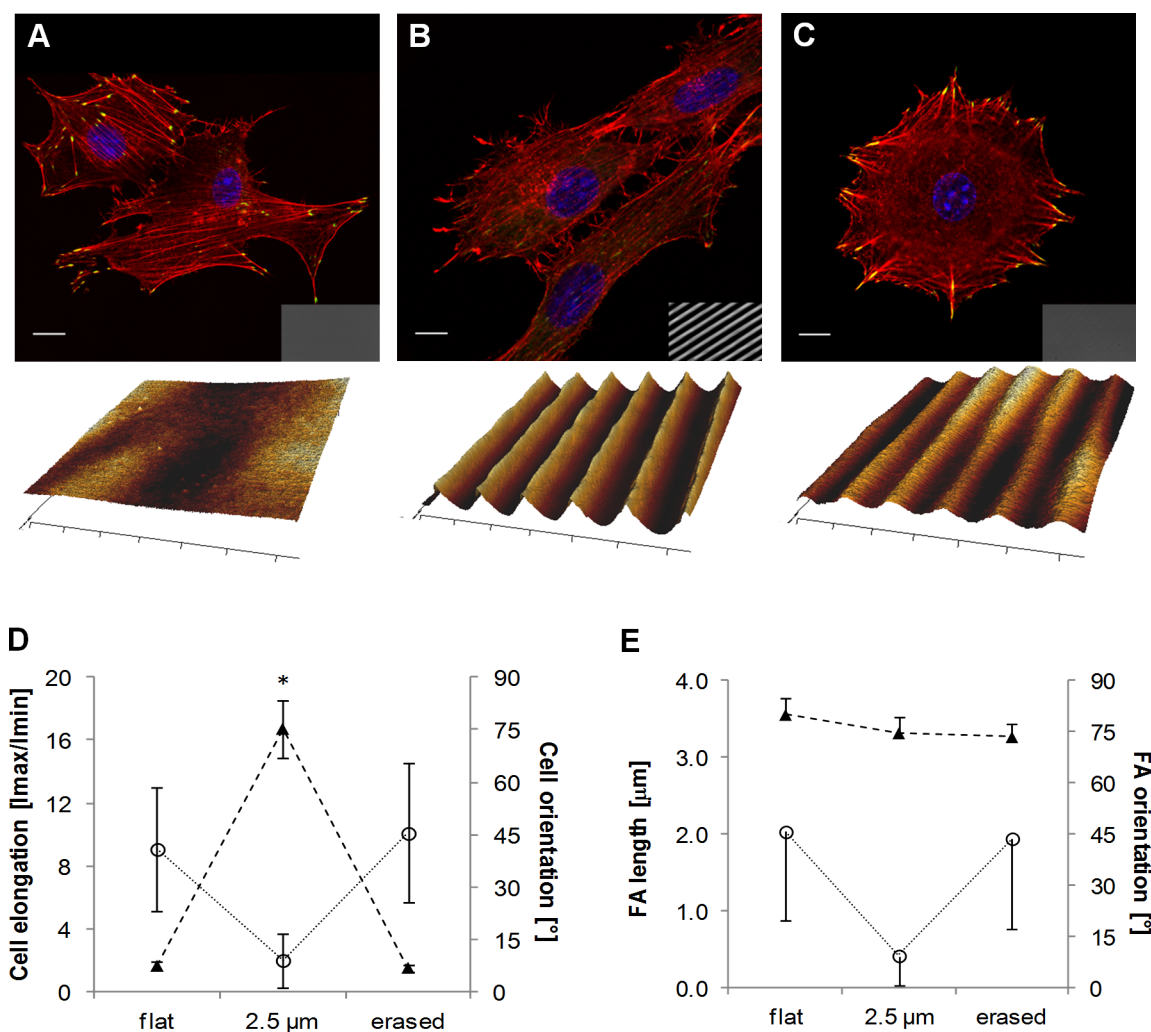


Figure 5. Confocal images of NIH-3T3 cells cultivated on (A) flat pDR1m substrate, (B) SRG grating, and (C) pattern erased with circularly polarized light. Transmission images of the substrate are reported in the bottom right corner of each confocal micrograph, and AFM scans are shown below them. (D) Plots of cell elongation (\blacktriangle) and cell orientation (\circ). (E) Plot of FA length (\blacktriangle) and orientation (\circ). The asterisk denotes a significant difference with respect to the flat case. Bars indicate the standard error of the mean in the case of cell elongation and FA length, whereas they represent the standard deviation in the case of cell and FA orientation.

cytoskeleton is also delayed. Stable actin bundels can form only a limited number of adhesion spots. The remaining actin is involved in an extensive ruffling at the cell periphery, as the cell tries to maximize the number of adhesions. Indeed, it is recognized that an increased ruffling activity occurs on scarcely adhesive substrates or when the available extracellular adhesive islets are very narrow.³³

Topographic patterns imprinted on pDR1m proved to be effective in controlling different aspects of the cell–material interactions and macroscopic cell behavior. More interestingly, though, surface modifications induced on azopolymers are, in principle, reversible; i.e., if they are exposed to specific chemical and physical cues, patterns can be manipulated or erased. Pattern erasure is an aspect that we carefully addressed as it would greatly increase the versatility of the pDR1m substrates. This could allow several instances of fabrication of various patterns on the same substrate without employing expensive equipment and further chemical products. In this work, pattern erasure was induced by using temperature or light as a trigger. In the first case, heating the linear SRG to 130 °C for 3 h caused the flattening of the gratings, and the pattern could be rewritten afterward (Figure 4).

Temperature erasure of SRGs cannot be directly applied to living cell cultures. However, thermal modification of the pattern allowed us to obtain a relatively smooth surface to which to compare the other manipulation techniques. In principle, photoswitching has the potential to be implemented for dynamic changes of the pattern features. As a preliminary experiment, circularly polarized light was used to reduce SRG depth. After irradiation for 10 min in air at room temperature, the grating depth decreased from 90 to 10 nm, similar in shape to that obtained through thermal processing. To assess the effectiveness of pattern modification on a cell culture experiment, we first cultivated NIH-3T3 cells on flat surfaces for 24 h. Cells were then trypsinized, and the substrates were washed in PBS and air-dried. Second, a 2.5 μm pattern was inscribed using the setup previously described on which cells were seeded on the patterned substrate and cultivated for 24 h. Finally, cells were trypsinized, the substrate was washed and dried, and the pattern was erased by exposing it to a circularly polarized light for 10 min at room temperature. To draw out quantitative data on cell morphology and adhesion, we prepared a second set of samples in which cells were fixed and stained rather than detached from each substrate with

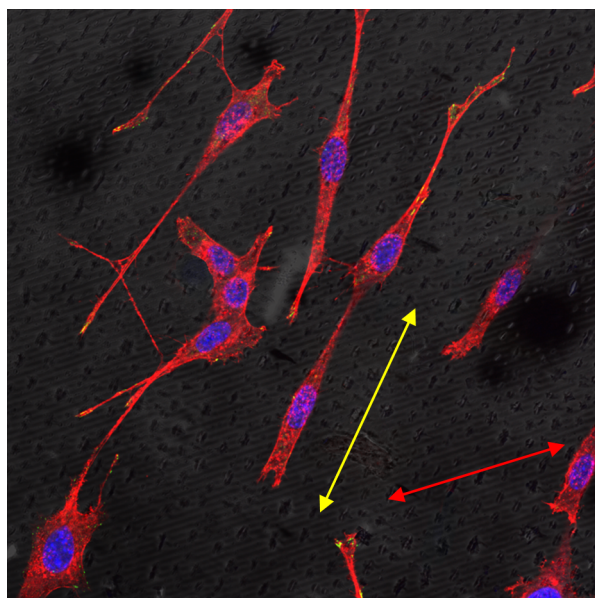


Figure 6. Confocal image of NIH-3T3 cells cultivated on a SRG pattern exposed to circularly polarized light in DMEM. The red arrow shows the original pattern direction, whereas the yellow arrow indicates the pattern of the newly formed bubblelike structure, induced by circularly polarized light.

trypsin. Therefore, confocal images of cells stained for vinculin, actin, and nuclei were acquired (Figure 5). Cells were randomly distributed on a flat polymer, while they acquired an elongated morphology when they were seeded on the linear pattern. Circularly polarized light dramatically reduced pattern height, and cells recovered a round morphology accordingly. The quantification of cell elongation and orientation is reported in Figure 5D, in which the highest values of elongation are measured on the $2.5\ \mu\text{m}$ pattern, whereas the elongation of cells on the erased pattern is not significantly different from that of the flat case. Accordingly, cell orientation was nearly parallel to the pattern direction with a narrow distribution when cells were seeded on the pattern, while a random orientation with a broad distribution was measured for cells on both flat and erased pattern. FA length did not display changes in the writing/erasing cycles, whereas FA orientation was very sensitive to the topography as parallel FAs were observed on the SRG only (Figure 5E). Therefore, pDR1m-coated substrates can in principle be rewritten with different patterns, and cells respond to the modified signal accordingly.

Cells are necessarily cultivated in aqueous media. To implement light-induced pattern modification or erasure while living cells are cultivated on the substrate, the circularly polarized laser beam must pass through the culturing medium before colliding onto the patterned surface. We then investigated whether the process of pattern erasure was affected by the presence of an aqueous environment. Therefore, the laser beam was directed into the Petri dish containing the SRG sample immersed in either water, PBS, or DMEM (1.5 mL in volume). After exposure for 10 min, we observed the formation of bubblelike structures on the polymer surface, which were arranged in a sort of aligned pattern. Simultaneously, the original topographic pattern intensity was drastically reduced. This particular effect occurred in a manner independent of the fluid type (see Figure S2 of the Supporting Information). As shown in Figure 6, cells seeded on the erased SRG were not able to perceive the original topographic signals (red arrow) but rather co-aligned along the bubblelike structures (yellow arrow).

The use of circularly polarized light to erase or reduce the pattern depth entailed a great disadvantage; in fact, the optical setup was hardly adaptable to cell environment conditions, and the laser intensity was not suitable for dynamic real-time experiments with cells. For this reason, we introduced a new approach to erase SRG structures on pDR1m films, based on the use of a microscope. This new strategy was more adaptable to biological conditions; in fact, because of the microscope equipment it was possible to identify precisely the polymer surface, and because of the coupled isolated thermo-chamber, the biological environment was easily reproduced, allowing the observation of cells over several hours after light exposure. In this case, an incoherent and unpolarized light beam of a mercury lamp, implemented in a Leica confocal microscope (15 mW intensity, 488 nm filter), was used to erase the patterns. In fact, incoherent and unpolarized light is highly effective in randomizing azobenzene molecule orientation, as well as circularly polarized light.³⁴

Starting from these observations, we irradiated a cell-populated $2.5\ \mu\text{m}$ pattern for 2 min with the mercury lamp. Also in this case, bubblelike structures appeared. However, NIH-3T3 cells were still vital and migrated over the substrate (Figure 7A–C and Video 1 of the Supporting Information).

Despite the fact that both circularly polarized and incoherent light sources proved to be very effective in erasing the pattern under dry conditions, the presence of an aqueous environment generates the bubblelike structures due to either scattering of the light or promotion of uncontrolled interactions between

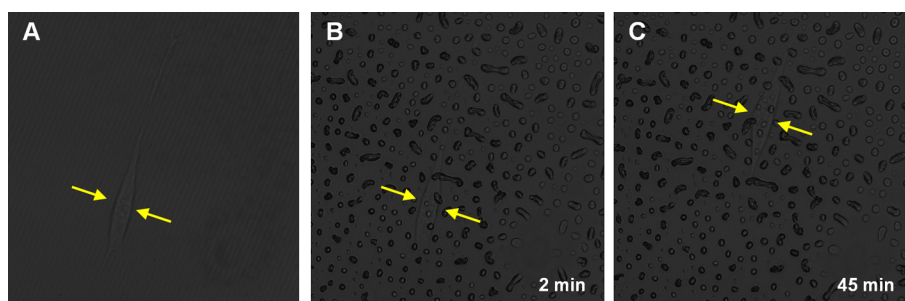


Figure 7. Live pattern erasure with a mercury lamp. Montage of confocal images of (A) a single cell migrating along the original $2.5\ \mu\text{m}$ pattern and (B) the same location acquired after the 2 min exposure of the incoherent light and (C) after 45 min. Yellow arrows indicate the cell body at the nuclear position.

water and the azopolymer. It is most likely that upon irradiation water molecules deform the polymer, while pDR1m is stable in aqueous media under the normal cell culturing conditions. Therefore, we hypothesize that a photofluidization process (athermal anisotropic photosoftening) occurs, meaning that light-induced molecule mobility allows small forces to generate material flow.³⁵ In an aqueous environment, this phenomenon triggers a sort of interfacial phase separation between the hydrophobic polymer and the aqueous environment, with the formation of globular polymeric domains on the substrates. However, this needs to be confirmed with specific experiments.

Azobenzene compounds, along with their response to light irradiation, have been widely investigated and are mainly used in the optics and photonics fields. Despite their extraordinary chemical and physical characteristics, the number of studies on the use of azobenzene-based substrates for cell cultures is limited. Specifically functionalized azopolymers were used to alter the surface chemistry of cell culture substrates, for example, wettability or ligand presentation, thus altering the cell response.³⁶ Azopolymers are particularly suitable for the fabrication of topographic patterns because of the orderly mass migration induced by interference patterns of linearly polarized light.¹³ This makes these polymers an ideal platform for studying cell–topography interactions. The topographic signal and in particular micron- and submicron-scale signals proved to strongly affect and control a specific aspect of the cell behavior. They finely regulate the processes of cell adhesion and migration,^{22,23,37} and topographies can exert a profound impact on cell differentiation^{2,5} and tissueogenesis.^{21,38} In the case of topographic patterns encoded on azopolymers for in vitro cell cultures, Rocha et al.¹⁹ studied the biocompatibility of azopolymer-based polysiloxane coatings and investigated the stability of the substrates in an aqueous environment. Barille et al.¹⁸ examined the imprinting capabilities of the azo-based photoswitchable materials under both dry and wet conditions and analyzed neuron response to the topographic signal. Interestingly, they also reported that irregularities were observed when the pattern was embossed in the presence of PBS. To the best of our knowledge, however, the possibility of exploiting the writing/erasing reversibility of azobenzene polymers in biological applications has not yet been addressed. We demonstrated that pDR1m-coated glass can be patterned in a reversible manner using either temperature or light triggers. Additionally, the microscopy setup we propose allows pattern feature alteration in the presence of cells without affecting their viability. However, even though the system has the potential to be employed for real-time experiments with living cells, the irradiation technique needs to be optimized to gain better control of azopolymer mass transport and hence improve pattern modification.

4. CONCLUSIONS

In this work, we presented an effective and inexpensive technique for imprinting and modifying large-scale biocompatible topographic patterns on pDR1m-coated glass, using conventional equipment. Patterned substrates proved to be effective in confining FA growth and cytoskeletal assembly. The pattern could be easily erased and rewritten under dry conditions, whereas in a wet environment, circularly polarized or incoherent light was able to alter pattern shape. In particular, incoherent and unpolarized light-mediated erasure proved to be a promising strategy for real-time experiments with living cells as microscopy setup and illumination exposure time did not

affect cell viability. Therefore, the system we proposed has the potential to be employed for understanding cell behavior and possibly mechanotransduction events in a dynamic environment.

■ ASSOCIATED CONTENT

Supporting Information

UV–vis absorption spectrum of pDR1m, AFM images and relative cross sections of SRG under dry conditions and after 24 h in DMEM at 37 °C, transmission images of SRGs exposed to circularly polarized light under wet conditions, and a video showing pattern erasure in the presence of a cell. This material is available free of charge via the Internet at <http://pubs.acs.org>.

■ AUTHOR INFORMATION

Corresponding Author

*E-mail: nettipa@unina.it.

Notes

The authors declare no competing financial interest.

■ ACKNOWLEDGMENTS

We thank Dr. Carlo F. Natale for the helpful suggestions on cell culturing and staining, Dr. Fabio Formiggini for his support in confocal image acquisition, Ms. Chiara Fedele for her support in pattern manipulation, and Ms. Valentina La Tilla for figure editing.

■ REFERENCES

- (1) Walboomers, X.; Croes, H.; Ginsel, L.; Jansen, J. Growth Behavior of Fibroblasts on Microgrooved Polystyrene. *Biomaterials* **1998**, *19*, 1861–1868.
- (2) McNamara, L. E.; McMurray, R. J.; Biggs, M. J.; Kantawong, F.; Oreffo, R. O.; Dalby, M. J. Nanotopographical Control of Stem Cell Differentiation. *J. Tissue Eng.* **2010**, *1*, 120623.
- (3) Ladoux, B.; Nicolas, A. Physically Based Principles of Cell Adhesion Mechanosensitivity in Tissues. *Rep. Prog. Phys.* **2012**, *75*, 116601.
- (4) Biggs, M. J. P.; Richards, R. G.; Dalby, M. J. Nanotopographical Modification: A Regulator of Cellular Function through Focal Adhesions. *Nanomedicine* **2010**, *6*, 619–633.
- (5) Yim, E. K.; Darling, E. M.; Kulangara, K.; Guilak, F.; Leong, K. W. Nanotopography-Induced Changes in Focal Adhesions, Cytoskeletal Organization, and Mechanical Properties of Human Mesenchymal Stem Cells. *Biomaterials* **2010**, *31*, 1299–1306.
- (6) Ventre, M.; Valle, F.; Bianchi, M.; Biscarini, F.; Netti, P. A. Cell Fluidics: Producing Cellular Streams on Micropatterned Synthetic Surfaces. *Langmuir* **2012**, *28*, 714–721.
- (7) Hallab, N.; Bundy, K.; O'Connor, K.; Clark, R.; Moses, R. Cell Adhesion to Biomaterials: Correlations between Surface Charge, Surface Roughness, Adsorbed Protein, and Cell Morphology. *J. Long-Term Eff. Med. Implants* **1994**, *5*, 209–231.
- (8) Flemming, R.; Murphy, C.; Abrams, G.; Goodman, S.; Nealey, P. Effects of Synthetic Micro- and Nano-Structured Surfaces on Cell Behavior. *Biomaterials* **1999**, *20*, 573–588.
- (9) Yeung, T.; Georges, P. C.; Flanagan, L. A.; Marg, B.; Ortiz, M.; Funaki, M.; Zahir, N.; Ming, W.; Weaver, V.; Janmey, P. A. Effects of Substrate Stiffness on Cell Morphology, Cytoskeletal Structure, and Adhesion. *Cell Motil. Cytoskeleton* **2005**, *60*, 24–34.
- (10) Ventre, M.; Causa, F.; Netti, P. A. Determinants of Cell–Material Crosstalk at the Interface: Towards Engineering of Cell Instructive Materials. *J. R. Soc., Interface* **2012**, *9*, 2017–2032.
- (11) Davis, K. A.; Burke, K. A.; Mather, P. T.; Henderson, J. H. Dynamic Cell Behavior on Shape Memory Polymer Substrates. *Biomaterials* **2011**, *32*, 2285–2293.
- (12) Le, D. M.; Kulangara, K.; Adler, A. F.; Leong, K. W.; Ashby, V. S. Dynamic Topographical Control of Mesenchymal Stem Cells by

Culture on Responsive Poly(ϵ -caprolactone) Surfaces. *Adv. Mater. (Weinheim, Ger.)* **2011**, *23*, 3278–3283.

(13) Natansohn, A.; Rochon, P. Photoinduced Motions in Azo-Containing Polymers. *Chem. Rev.* **2002**, *102*, 4139–4176.

(14) Rochon, P.; Batalla, E.; Natansohn, A. Optically Induced Surface Gratings on Azoaromatic Polymer Films. *Appl. Phys. Lett.* **1995**, *66*, 136–138.

(15) Kim, D.; Tripathy, S.; Li, L.; Kumar, J. Laser-Induced Holographic Surface Relief Gratings on Nonlinear Optical Polymer Films. *Appl. Phys. Lett.* **1995**, *66*, 1166–1168.

(16) Marder, S. R.; Kippelen, B.; Jen, A. K.-Y.; Peyghambarian, N. Design and Synthesis of Chromophores and Polymers for Electro-Optic and Photorefractive Applications. *Nature* **1997**, *388*, 845–851.

(17) Priimagi, A.; Shevchenko, A. Azopolymer-Based Micro- and Nanopatterning for Photonic Applications. *J. Polym. Sci., Part B: Polym. Phys.* **2014**, *52*, 163–182.

(18) Barillé, R.; Janik, R.; Kucharski, S.; Eyer, J.; Letournel, F. Photo-Responsive Polymer with Erasable and Reconfigurable Micro- and Nano-Patterns: An In Vitro Study for Neuron Guidance. *Colloids Surf., B* **2011**, *88*, 63–71.

(19) Rocha, L.; Păiuș, C.-M.; Luca-Raicu, A.; Resmerita, E.; Rusu, A.; Moleavin, I.-A.; Hamel, M.; Branza-Nichita, N.; Hurduc, N. Azobenzene Based Polymers as Photoactive Supports and Micellar Structures for Applications in Biology. *J. Photochem. Photobiol., A* **2014**, *291*, 16–25.

(20) Baac, H.; Lee, J.-H.; Seo, J.-M.; Park, T. H.; Chung, H.; Lee, S.-D.; Kim, S. J. Submicron-Scale Topographical Control of Cell Growth Using Holographic Surface Relief Grating. *Mater. Sci. Eng., C* **2004**, *24*, 209–212.

(21) Iannone, M.; Ventre, M.; Formisano, L.; Casalino, L.; Patriarca, E. J.; Netti, P. A. Nanoengineered Surfaces for Focal Adhesion Guidance Trigger Mesenchymal Stem Cell Self-Organization and Tenogenesis. *Nano Lett.* **2015**, *15*, 1517–1525.

(22) Natale, C. F.; Ventre, M.; Netti, P. A. Tuning the Material-Cytoskeleton Crosstalk via Nanoconfinement of Focal Adhesions. *Biomaterials* **2014**, *35*, 2743–2751.

(23) Ventre, M.; Natale, C. F.; Rianna, C.; Netti, P. A. Topographic Cell Instructive Patterns to Control Cell Adhesion, Polarization and Migration. *J. R. Soc., Interface* **2014**, *11*, 20140687.

(24) Jiang, X.; Li, L.; Kumar, J.; Kim, D.; Tripathy, S. Unusual Polarization Dependent Optical Erasure of Surface Relief Gratings on Azobenzene Polymer Films. *Appl. Phys. Lett.* **1998**, *72*, 2502–2504.

(25) Schindelin, J.; Arganda-Carreras, I.; Frise, E.; Kaynig, V.; Longair, M.; Pietzsch, T.; Preibisch, S.; Rueden, C.; Saalfeld, S.; Schmid, B. Fiji: An Open-Source Platform for Biological-Image Analysis. *Nat. Methods* **2012**, *9*, 676–682.

(26) Yager, K. G.; Barrett, C. J. Temperature Modeling of Laser-Irradiated Azo-Polymer Thin Films. *J. Chem. Phys.* **2004**, *120*, 1089–1096.

(27) Barrett, C. J.; Natansohn, A. L.; Rochon, P. L. Mechanism of Optically Inscribed High-Efficiency Diffraction Gratings in Azo Polymer Films. *J. Phys. Chem.* **1996**, *100*, 8836–8842.

(28) Pedersen, T. G.; Johansen, P. M.; Holme, N. C. R.; Ramanujam, P.; Hvilsted, S. Mean-Field Theory of Photoinduced Formation of Surface Reliefs in Side-Chain Azobenzene Polymers. *Phys. Rev. Lett.* **1998**, *80*, 89.

(29) Kumar, J.; Li, L.; Jiang, X. L.; Kim, D.-Y.; Lee, T. S.; Tripathy, S. Gradient Force: The Mechanism for Surface Relief Grating Formation in Azobenzene Functionalized Polymers. *Appl. Phys. Lett.* **1998**, *72*, 2096–2098.

(30) Bian, S.; Liu, W.; Williams, J.; Samuelson, L.; Kumar, J.; Tripathy, S. Photoinduced Surface Relief Grating on Amorphous Poly(4-phenylazophenol) Films. *Chem. Mater.* **2000**, *12*, 1585–1590.

(31) Hurduc, N.; Donose, B. C.; Macovei, A.; Paius, C.; Ibanescu, C.; Scutaru, D.; Hamel, M.; Branza-Nichita, N.; Rocha, L. Direct Observation of Athermal Photofluidisation in Azo-Polymer Films. *Soft Matter* **2014**, *10*, 4640–4647.

(32) Biela, S. A.; Su, Y.; Spatz, J. P.; Kemkemer, R. Different Sensitivity of Human Endothelial Cells, Smooth Muscle Cells and

Fibroblasts to Topography in the Nano–Micro Range. *Acta Biomater.* **2009**, *5*, 2460–2466.

(33) Lutz, R.; Pataky, K.; Gadhari, N.; Marelli, M.; Brugger, J.; Chiquet, M. Nano-stenciled RGD-gold Patterns that Inhibit Focal Contact Maturation Induce Lamellipodia Formation in Fibroblasts. *PLoS One* **2011**, *6*, e25459.

(34) Yager, K. G.; Barrett, C. J. In *Polymeric Nanostructures and Their Applications*; Nalwa, H. S., Ed.; American Scientific Publishers: Valencia, CA, 2006; Chapter 8, pp 1–38.

(35) Karageorgiev, P.; Neher, D.; Schulz, B.; Stiller, B.; Pietsch, U.; Giersig, M.; Brehmer, L. From Anisotropic Photo-Fluidity Towards Nanomanipulation in the Optical Near-Field. *Nat. Mater.* **2005**, *4*, 699–703.

(36) Wang, G.; Zhang, J. Photoresponsive Molecular Switches for Biotechnology. *J. Photochem. Photobiol., C* **2012**, *13*, 299–309.

(37) Seo, C. H.; Jeong, H.; Furukawa, K. S.; Suzuki, Y.; Ushida, T. The Switching of Focal Adhesion Maturation Sites and Actin Filament Activation for MSCs by Topography of Well-Defined Micropatterned Surfaces. *Biomaterials* **2013**, *34*, 1764–1771.

(38) Kim, D. H.; Lipke, E. A.; Kim, P.; Cheong, R.; Thompson, S.; Delannoy, M.; Suh, K. Y.; Tung, L.; Levchenko, A. Nanoscale Cues Regulate the Structure and Function of Macroscopic Cardiac Tissue Constructs. *Proc. Natl. Acad. Sci. U.S.A.* **2010**, *107*, 565–570.